Wave-optical experiments with very cold neutrons

Roland Gähler
Physikdepartment E21, Technische Universität München, D-8046 Garching, Germany

Anton Zeilinger
Institut für Experimentalphysik, Universität Innsbruck, Technikerstrasse 25, A-6020 Innsbruck, Austria, and Atominstitut der Österreichischen Universitäten, Schüttelstrasse 115, A-1020 Wien, Austria

(Received 14 November 1990; accepted for publication 26 November 1990)

A series of experiments is reviewed on precision measurements of the diffraction of slow neutrons paralleling those with light: diffraction at an absorbing edge, at an absorbing wire, and at single- and double-slit assemblies. Besides their educational value, the experimental results also provide precise confirmations of the theoretical predictions as calculated via a Fresnel–Kirchhoff approach. The intensity in all these experiments was so low that the formation of the interference patterns individual neutron by individual neutron could easily be observed. The experiments are presented and analyzed in a way suitable for undergraduate teaching.

I. INTRODUCTION

One of the greatest achievements of physics in this century is the discovery of the wave nature of matter through the experimental work of Davisson and Germer.[1] A discovery which, incidentally, was made independently from the proposal of Louis de Broglie.[2] Today, experimental evidence for the wave nature of matter is abundant, yet it is always interesting and instructive to study diffraction of matter waves at simple geometric objects. It is the purpose of the present paper to review a series of such experiments[3] performed with cold neutrons over recent years and to present and analyze them in a way suitable for introductory physics courses. The experiments are complete analogs to the classic wave-optical experiments with light: diffraction at an absorbing edge, at an absorbing wire, and at single- and double-slit assemblies. When introducing the wave nature of matter to students, diffraction of electrons at crystals is often presented as typical experimental evidence. We propose that the use of results of the type presented here will provide evidence that is more readily accessible to students at an early stage because only concepts already known from standard light optics are used for their explanation. The experiments are so fundamentally simple that they might even be presented in the introductory teaching of the phenomenon of diffraction itself.

The experiments also complement earlier analogous work with electrons.[4] In comparison with electrons, experiments with neutrons are better suited for high-precision experimental studies. This is a consequence of the electric neutrality of the neutron and the smallness of its magnetic moment. Both features imply that laboratory stray electric and magnetic fields are of much lower disturbing influence on the diffraction patterns and hence precision comparison with theory is easier to achieve. It is noteworthy that with electrons the double-slit experiment has already found experimental verification in the 50s[5] and it is rather disturbing that in many textbooks diffraction of electrons at double-slit assemblies still is presented as a gedanken experiment. Its various experimental realizations go largely unnoticed as has been pointed out recently in this Journal.[6] Today there exists a significant tradition of experiments in the field of electron interferometry[7] and we have to refer the interested reader to the lists of references of the most recent papers quoted here. A number of the electron experiments have demonstrated explicitly that the interference pattern obtained is independent of the intensity of the electron beam. This is particularly interesting if the intensity is so low that one literally can watch the interference pattern building up through the accumulation of individual flashes on a screen, an experimental observation known already from the early days of electron interferometry experimentation.

The field of neutron interferometry started in the mid-70s[8] and has provided many demonstrations and tests of fundamental predictions of quantum mechanics.[9] For reasons of technical limitations of neutron sources available, experiments in that field had initially been performed with so-called thermal neutrons with wavelengths around 1 Å. Such wavelengths are too small to lead to clearly observable diffraction effects of the kind discussed here. The considerable improvement of sources for very cold neutrons (VCN) in the last decade has led to a significant increase of the intensities of slower, i.e., longer wavelength, neutron beams and thus has made the present work possible. It is instructive for the student to note that here, too, as in many areas of experimental science, advances in fundamental research are a consequence of earlier technological progress.

II. EXPERIMENTAL SETUP AND PROCEDURE

From the beginning, it was the purpose of our experiments to perform a precision study of the diffraction of neutrons by macroscopic objects whose dimensions can be determined by independent observation. As compared to electrons, a major advantage of neutrons for such precision experiments stems from their electric neutrality. This implies that neutrons are only very weakly—through their small magnetic moment—influenced by stray laboratory fields. This may also be in part an explanation for the fact that until today, to our knowledge, no precision comparison between an observed electron diffraction pattern and first-principles theoretical prediction has been done. For photons there exists a number of such experiments up to diffraction at objects of very large dimensions.[10]

The experiments were performed at the high-flux reactor of the Institute Laue–Langevin (ILL) in Grenoble, France, the best presently existing neutron source for such studies. In a nuclear reactor, the neutrons set free by the fission process have energies around 2 MeV, which corresponds to speeds around 20 000km/s. These neutrons are slowed down by collisions with the moderator nuclei to

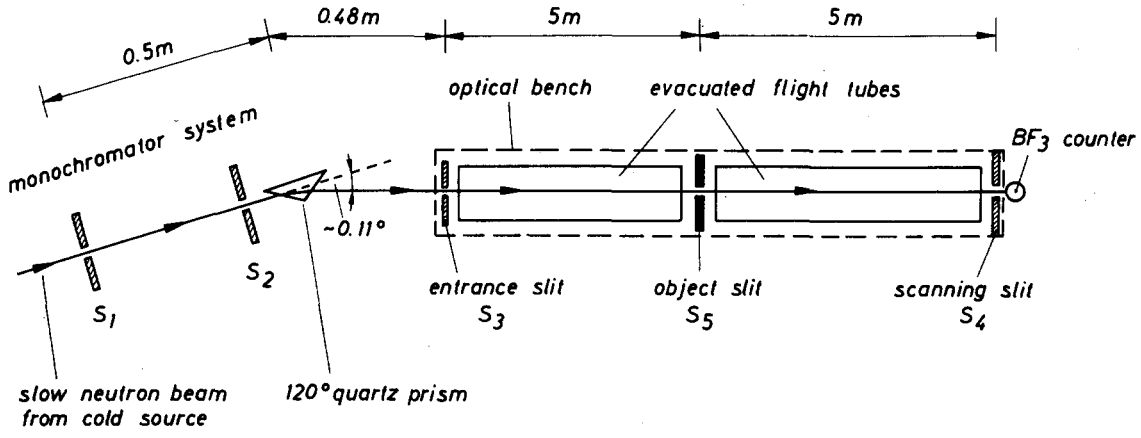

Fig. 1. Sketch of the experimental setup (not to scale). The neutrons coming from the cold source are monochromatized by prism refraction. The diffraction pattern produced by the diffracting object (object slit) is then measured by stepping the scanning slit through the observation plane.

thermal energies. Their energy distribution is thus Maxwellian with a temperature around 300 K, which, in turn implies neutron speeds v around 2 km/s and de Broglie wavelengths $\lambda = h/mv$ around 2 Å (1 Å $= 10^{-10}$ m). Such wavelengths are just of the same order of magnitude as interatomic distances in condensed matter and this is one of the reasons for the broad application of neutrons in materials. Beams of neutrons with larger wavelengths necessary for experiments of the kind reported here are available at the ILL high-flux reactor as emerging from a cold source. The ILL cold source is a neutron moderator where the moderator material is liquid deuterium at a temperature around 25 K. Our experiment exploits the increase of the low-energy tail of the Maxwellian distribution of that temperature as compared to the customary room temperature situation.

The neutron beam from the cold source after passage through a curved guide entered a prism refraction monochromator system (Fig. 1). There the variable-width slit S_1 and the 100-μm-wide slit S_2 define the direction of the neutron beam incident on the prism. Because of the dispersive properties of the prism medium (quartz glass), for neutrons the radiation emerging behind the prism is fanned out exhibiting a correlation between wavelength and direction very much analogous to the rainbow-colored light radiation field emerging from a glass prism. In contrast to light, the neutron refractive index is smaller than unity for most materials. As a consequence the prism orientation in Fig. 2 is reversed as compared to the customary light case. The 20-μm-wide optical bench entrance slit S_3 then selects neutrons of a specific wavelength out of the radiation field emerging from the prism. Slit S_3 also serves in defining through slit diffraction the width of the coherent wave front in the object plane that is located after a further flight path of 5 m. After another 5 m of flight path the neutrons pass the 20-μm-wide scanning exit slit S_4 and enter the neutron detector. The entrance slit S_3, the scanning slit S_4, and the diffracting object were supported directly from an optical bench that was a previously annealed steel beam of 10.5-m length thermally isolated from the environment to minimize thermal bending.

The diffraction patterns were then measured by moving the scanning slit S_4 in steps through the observation plane and counting the number of neutrons transmitted through

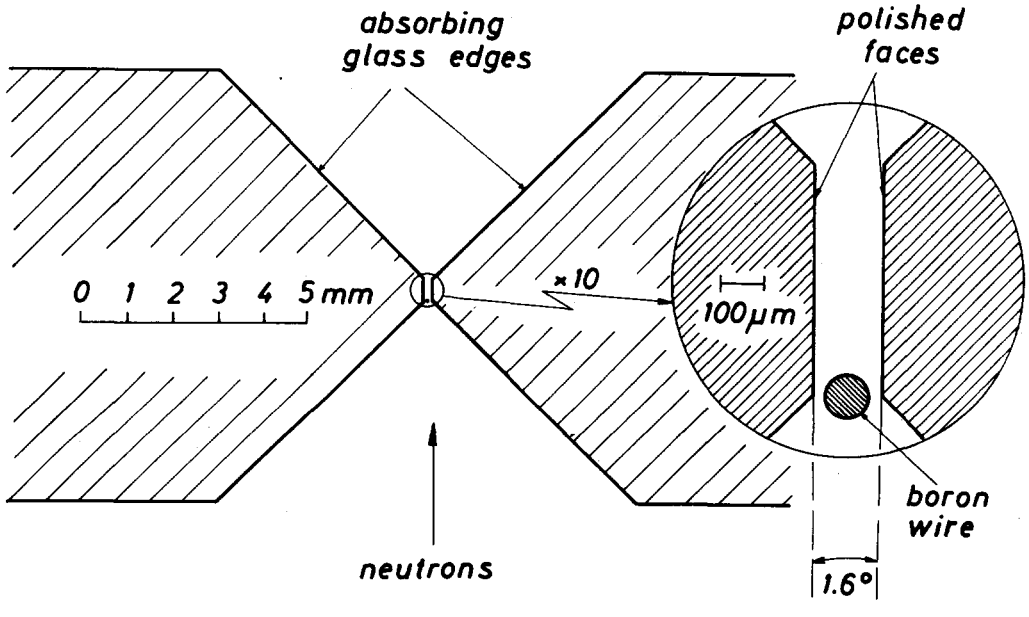

Fig. 2. Cross section through a slit assembly. A single slit is defined by the two absorbing glass edges and a double slit is then obtained by mounting a wire into that single slit. For the edge diffraction experiment only one glass edge was used.

that scanning slit to the neutron detector. The detector was a proportional chamber with BF_3 gas added. The neutrons are absorbed in the ^{10}B nuclei through the nuclear reaction $^{10}B + {}^1n \Rightarrow {}^7Li + {}^4\alpha$, where the reaction products finally produce the ionizations of the detector gas. It is worth noting that the efficiency of the detector can be adjusted by varying the concentration of the BF_3 gas and it can be made to approximate 100% efficiency in principle as closely as one wishes. In our experiment, the efficiency was adjusted to be about 90% for the very cold neutrons used. Because of the fact that in that wavelength range the neutron absorption cross section of boron is inversely proportional to the neutron speed, this implies a much smaller sensitivity to the thermal neutrons that constitute the major component to the background. As a result of this procedure and of careful shielding of the detector, the background count rate was as low as about 5 neutrons per hour.

By rotating the monochromator prism around its vertical axis and/or by repositioning the slit S_3, the wavelength of the neutrons could be varied between about 15 and 30 Å. It is customary in neutron physics to assign to a neutron beam a temperature through the relation $kT = mv^2/2$ even when the beam is not describable by a Maxwellian distribution.[11] For our beam that procedure would result in a temperature of a few tenths of a Kelvin; this is why such neutrons are termed very cold neutrons. In the experiment, the width of the wavelength band was adjusted by changing the width of the monochromator entrance slit S_1. The neutron velocity distribution was determined then by measuring the flight time of the neutrons along the full length of the optical setup. These measured velocity distributions were finally converted into wavelength distributions using the de Broglie relation

$$\lambda = h/mv$$

in its standard nonrelativistic form.

The exact values both of the mean wavelength and of the bandwidth used were varied for practical reasons from experiment to experiment. The mean wavelength was always of the order of 2 nm (or 20 Å) and the full-width wavelength bandwidth was varied between about 5% and 15%. All these numbers were determined with an error of about 0.1%. More precise numbers for the specific experiments will be given where appropriate.

All slit assemblies including the diffracting object (Fig. 2) were assembled using edge pieces precision manufactured from a special glass with high boron content to which 10 % Gd_2O_3 had been added to increase neutron absorption. Thus the resulting glass was virtually black for the neutrons used in our experiment.

The dimensions of the diffracting objects were primarily determined using a microscope traveling on a micrometer translation stage. This procedure resulted in an error in the dimensions which was typically between 0.3 and 0.5 μm. For the case of the slit-diffraction experiments, the slit width was also determined by measuring the thickness of steel sheet spacers used to define the slit gap opening. The results obtained by these procedures were consistent with each other. For more details of the alignment and measurement procedures and for considerations of the precision achieved we refer the reader to our original publications (Ref. 3).

In all the figures showing the experimental results the error bars exhibited are just the Poissonian standard deviations $\sqrt{N}$ when the total number of counted neutrons at a given position is N. The solid curve shown in all figures is the result of first-principles theoretical calculation; the fit was adjusted only by normalizing to give the correct *total intensity*. The calculation was done using the Fresnel–Kirchhoff formalism with all features of the experimental setup taken into account. These were the measured wavelength distribution, the angular divergence of the incident radiation, and the widths and positions of all slits used in the experiment. The integration over the latter was done coherently, i.e., the amplitudes over various paths were added and then squared to obtain the probability distribution. The sum over wavelength distribution and incident directional divergence was done incoherently, i.e., the intensities of the individual contributions were summed. For details of the calculation, the reader is referred to our original publications (Ref. 3).

For pedagogic reasons, in the present paper we will just give simple estimates of the magnitude of various features of the diffraction patterns but the reader should always keep in mind that the curves shown in the figures were obtained using a complete theoretical approach.

III. DIFFRACTION AT AN ABSORBING EDGE AND AT AN ABSORBING WIRE

The first experiment performed concerned the measurement of the diffraction at an absorbing straight edge. This experiment was aimed at testing hypothetical nonlinear variants of the Schrödinger equation. In the experiment we did not find any evidence for such nonlinearities; this result imposes rather stringent limits on any possible deviations from standard linear quantum mechanics.

Figure 3 shows the measured neutron distribution and we may in a very simple way estimate a characteristic scale of the diffraction pattern by calculating the scale of the first Fresnel zone for our experiment.[12] This is

$$Y_0 = \sqrt{\lambda L},$$

where L is both the distance from the entrance slit to the diffracting object and the distance from the diffracting object to the observation screen, both these distances being equal in our experiment. With $L = 5$ m and the neutron wavelength $\lambda = 2$ nm we obtain for the scale of the first Fresnel zone the value $Y_0 = 100\,\mu$m. In any Fresnel edge diffraction pattern there are two distinctive points. One is the point P_0 which is just the position of the edge projected onto the observation screen. The intensity at that point is exactly 25% of the intensity level with no edge present, the latter being equivalent to the mean intensity of the pattern far away from the edge in the case of homogeneous illumination. The other distinctive point is the position of the first diffraction maximum. It is known from standard diffraction theory that the distance Y between these two points is just $Y = 1.22\,Y_0$. This is clearly the correct scale of the pattern exhibited in Fig. 3.

The diffraction at an absorbing wire is another classic optical experiment. In our case we used a wire made of boron with a diameter of 104 μm. Boron is black for the neutrons of our wavelength. Figure 4 shows the diffraction pattern obtained which, at first sight, seems to be just the combination of two Fresnel edge diffraction patterns resulting from the diffraction at the two edges of the wire. Yet, upon close inspection, various deviations from that pattern may be seen which result from interference between amplitudes having passed the wire at the two dif-

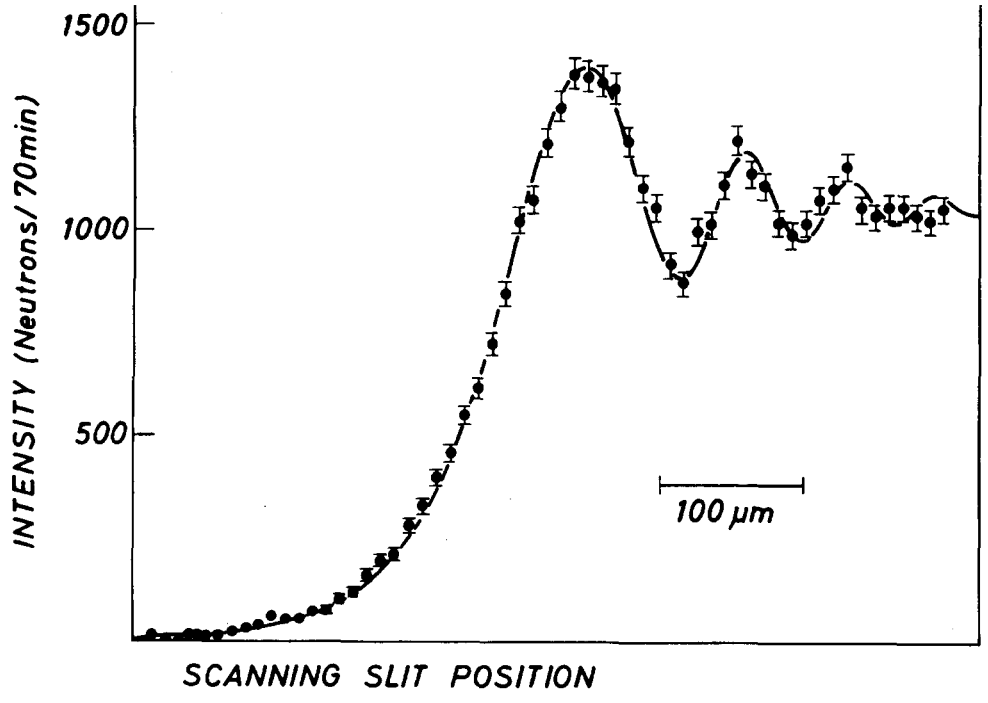

Fig. 3. Measured neutron distribution after diffraction at an absorbing edge. Here, and in all other figures, the solid line shows the theoretical prediction.

ferent sides. The most important feature is the small maximum in the center of the pattern. This is the famous Poisson's spot, the existence of which has been proposed in a *reductio ad absurdum* argument by Poisson against Fresnel's diffraction theory and which has been verified experimentally by Arago.[13] As is well known from optics, that spot arises in the center behind any diffracting object because symmetric optical paths leading along the different sides of the diffracting object to that center point are of equal length and, hence, their corresponding amplitudes interfere constructively. We may note here that Poisson's spot has also been verified very nicely for electron waves.[14]

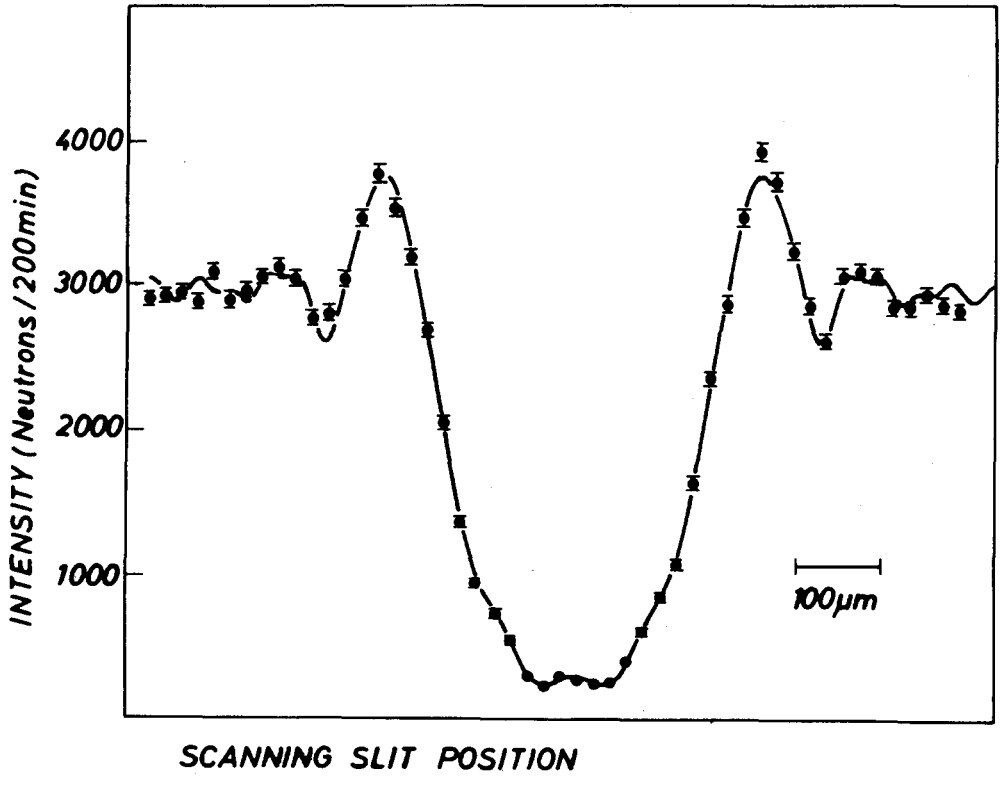

Fig. 4. Measured neutron distribution after diffraction at an absorbing wire. Note the small maximum in the center of the pattern. This is due to constructive interference of amplitudes passing the wire on both sides.

IV. SINGLE-SLIT DIFFRACTION

Experiments have been done of the diffraction at single slits of two different widths with neutrons of 19.26 Å mean wavelength. In the first experiment, a slit width of 93 μm was chosen so as to produce within the traveling range of 1 mm of the scanning slit a few well-resolved diffraction maxima on either side of the zero-order central maximum. For such a slit we calculate within the Fraunhofer[15] approximation for the angular separation between two diffraction minima,

$$\Delta\vartheta \approx \frac{(\lambda/2)}{(\delta/2)} = \frac{\lambda}{\delta} = \frac{(1.9\times10^{-9}\,\mathrm{m})}{(9\times10^{-5}\,\mathrm{m})} = 2.1\times10^{-5}\,\mathrm{rad},$$

where δ is the slit width. After a flight path of 5-m length this translates into a positional separation of 105 μm between the minima. Figure 5 shows the diffraction pattern obtained. Because of the broad width (1.4 Å) of the wavelength band used and because of geometric limitations, the minima between the zero-order central maximum and the two first-order maxima are not resolved. Nevertheless, the separation between the higher-order maxima is of the expected magnitude as inspection of Fig. 6 reveals. Figure 6 is just an enlargement of Fig. 5. Again, the solid line here represents the first-principles calculation.[16]

In another single-slit diffraction experiment, the slit width was chosen such that a precise observation of just the broadening of the zero-order central maximum due to slit diffraction was possible. For that purpose, the slit width was changed to 23 μm. The width of the zero-order diffraction maximum may again be estimated in a simple way by noting that as a consequence of Heisenberg's uncertainty relation any positional definition always leads to related momentum uncertainty $\Delta p \approx h/\Delta x$. In our case, passage through the slit of width δ implies a momentum uncertainty of the order of $\Delta p \approx h/\delta$. This in turn results in an uncertainty of the propagation direction of

$$\Delta\vartheta \approx \frac{(h/\delta)}{(h/\lambda)} = \frac{\lambda}{\delta} = \frac{(1.9\times10^{-9}\,\mathrm{m})}{(2.3\times10^{-5}\,\mathrm{m})} = 8.3\times10^{-5}\,\mathrm{rad}.$$

After a flight path of 5 m this implies a mean width of the spatial distribution of the neutrons of the order of

$$\Delta X \approx (5\,\mathrm{m})\times(8.3\times10^{-5}) = 415\,\mu\mathrm{m}.$$

It is evident that considerations of that kind can only give a rough estimate of the width of the diffraction pattern. Yet inspection of Fig. 7 indeed reveals that the full width at half maximum of the zero-order diffraction peak is just of that magnitude.

V. DOUBLE-SLIT DIFFRACTION

As pointed out already above, diffraction at a double-slit assembly is presented in many textbooks as *the* fundamental *gedanken* experiment when the wave properties of matter are introduced and particularly when one attempts to discuss the evidence for wave–particle duality. It is therefore clearly a challenge to the experimentalist to realize that experiment in the laboratory for many different types of particles and with the highest possible precision. In the course of the experiments reviewed here we did perform two experiments of the diffraction of neutrons at double-slit assemblies. The two experiments performed both used a wide single slit made of absorbing glass edges into whose gap a wire was mounted such as to obtain two well-separated smaller slits. The two experiments differed by the wire

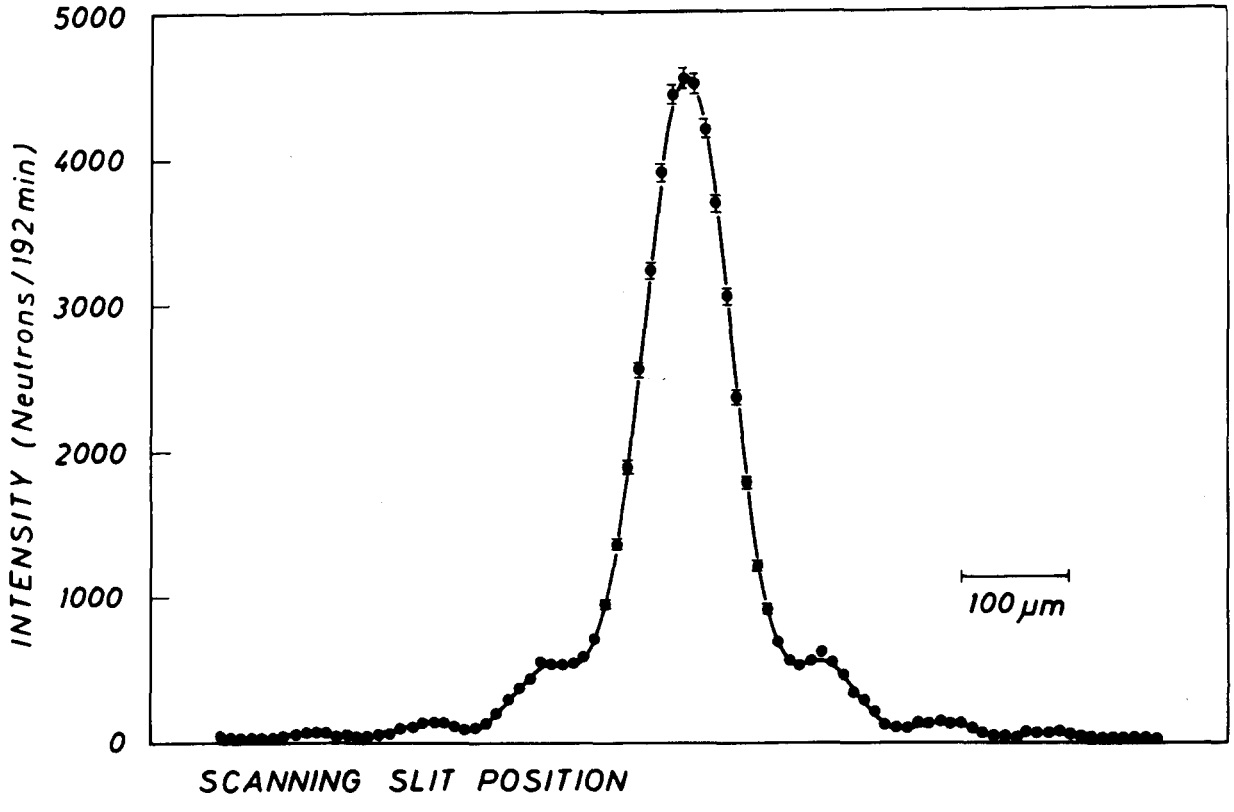

Fig. 5. Measured neutron distribution after diffraction at a single slit of 93-μm width.

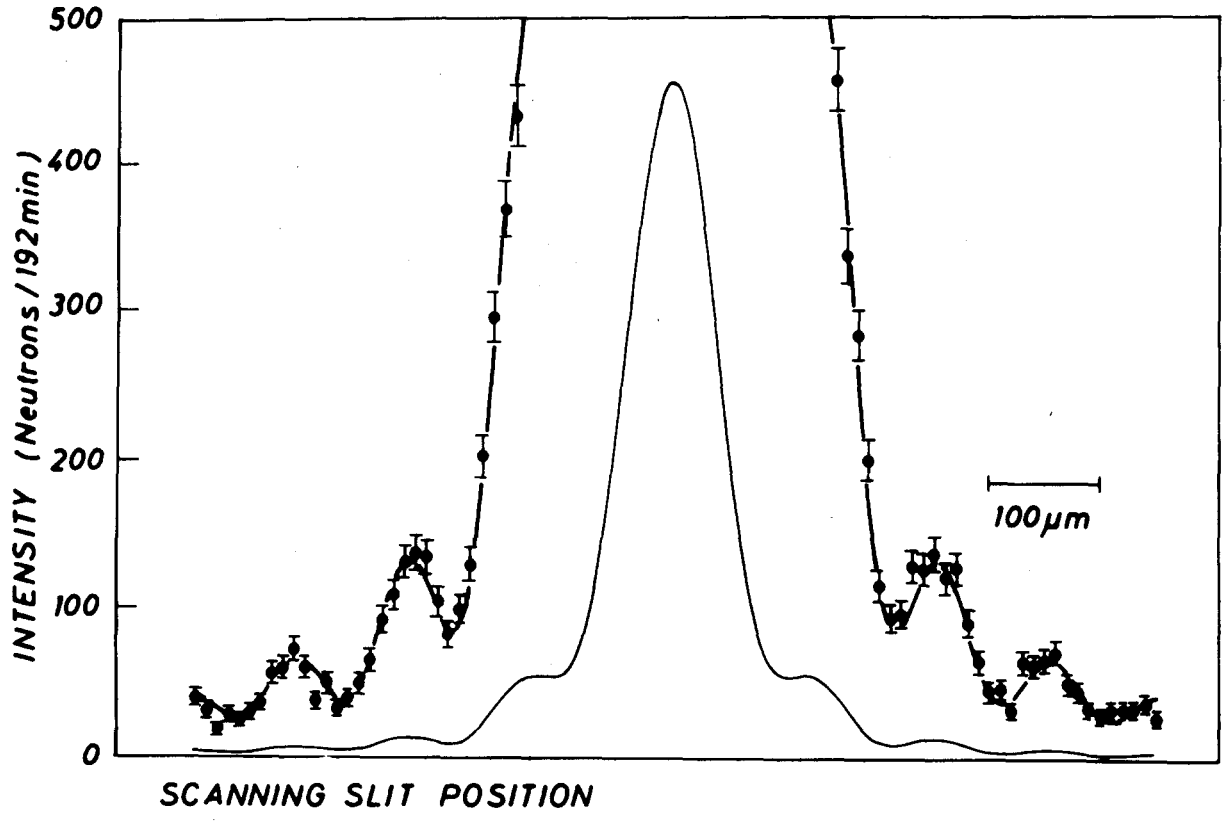

Fig. 6. Measured neutron distribution after diffraction at the 93-μm-wide single slit, enlarged to show the maxima of second, third, and, partly, fourth order. The solid curve is the same theoretical calculation as that of Fig. 5. Note the excellent agreement between theory and experiment at the higher-order maxima.

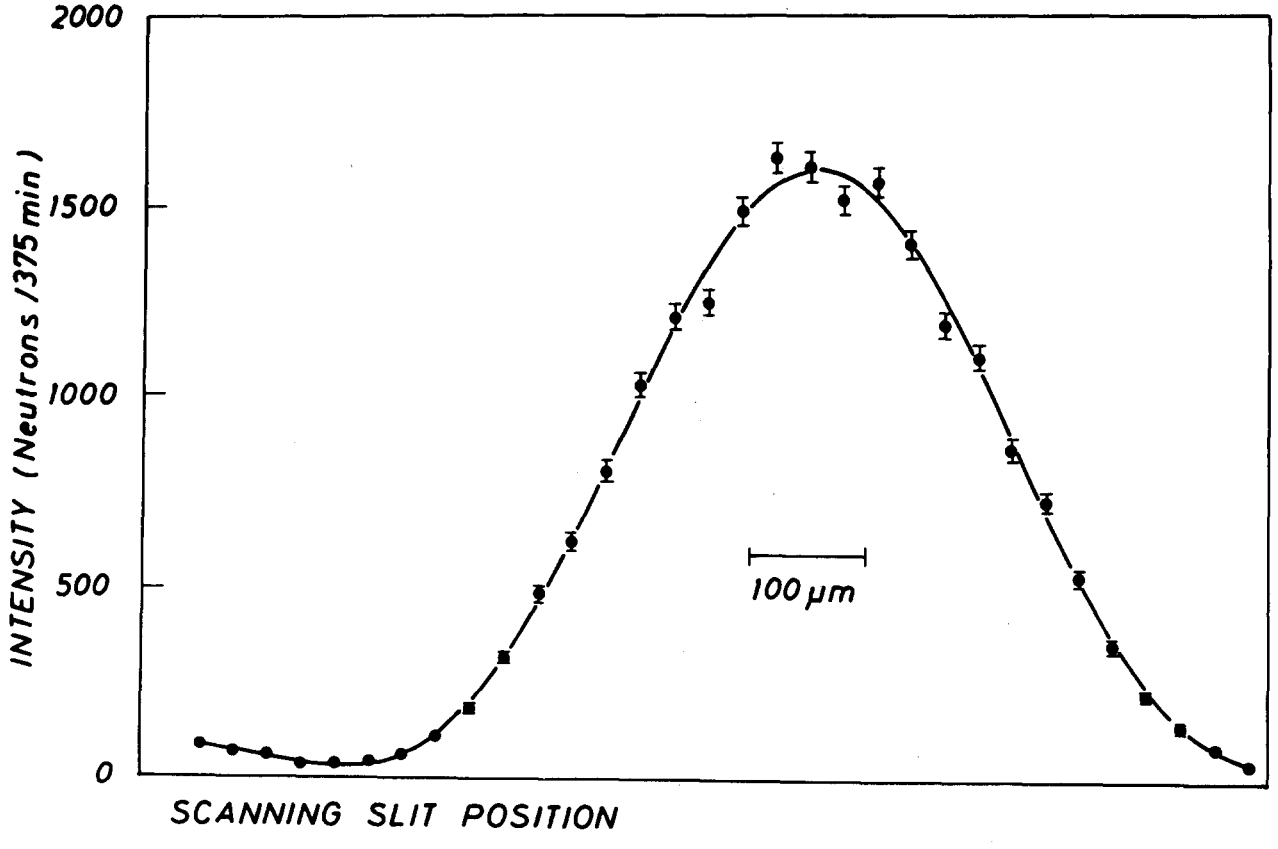

Fig. 7. Measured neutron distribution after diffraction at a single slit of 23-μm width. Note the broadening of the zero-order maximum, i.e., the loss in momentum definition, as expected because of the higher positional definition as compared to the broader slit above.

material used. In one experiment this was gold which, though being usually regarded as a strong absorber for neutrons, is practically transparent (absorption only ca 5%) at the low wire thickness used in the experiment. Thus, in our case, the gold wire acts essentially as a phase shifter for the neutrons as will be discussed below in more detail. This is to be contrasted with the second double-slit experiment reported here where the wire mounted into the wide slit was made of boron. That wire was opaque for the neutrons and thus the neutrons could only pass through either of the smaller slit openings left unobstructed on either side of the wire. Figure 2 shows the slit assembly in cross section with the boron wire mounted between the slit edges. We would like to stress that both double-slit assemblies used were of macroscopic dimensions in the sense that with the bare eye one could easily discriminate two well-separated slits, as inspection of the dimensions given in Fig. 2 confirms.

The gold wire used in the first experiment had a thickness of 61.4 μm and was mounted into a broad slit of 108.5-μm width thus leaving two slits open, each about 24 μm wide. The diffraction pattern of that arrangement has to be calculated by taking into account the phase shift experienced by the neutron along the various trajectories through the gold wire. The phase shift $\Delta\chi$ along a trajectory of length Δx is related to the neutron refractive index n via

$$\Delta\chi = (n-1)k \times \Delta x,$$

where $k = 2\pi/\lambda$. The neutron refractive index is related to the coherent scattering length b_c of the nuclei[17] and this finally leads to

$$\Delta\chi = -N\lambda b_c\, \Delta x,$$

with N being the number of nuclei per unit volume. For our case, this phase shift had to be calculated along all possible trajectories through the gold wire and the amplitudes of the individual trajectories were then coherently superposed taking the small absorption in the wire into account. In order to give an indication of the magnitudes of the phase shifts involved, we mention that for the wavelength used in our experiment passage of the neutrons through 4.8 μm of gold results in a phase shift of 2π. The neutron wavelength distribution in that experiment agreed with that used in the single-slit experiments. Figure 8 exhibits the experimental results together with the theoretical calculation. We note that the agreement is excellent with a coherent scattering length for gold of $b_c = 0.757$ fm for the best fit that agrees within experimental error with the recommended best value of $b_c = 0.763 \pm 0.006$ fm.[18]

In contrast to the experiment just discussed, the analysis of the double-slit experiment with boron wire did not have to take into account any neutrons transmitted through the wire. This is because the boron wire was opaque for neutrons of the wavelength used. In that experiment, the mean neutron wavelength was 18.45 Å. Due to difficulties in mounting the boron wire exactly centered, the two resulting slits were slightly unequal, 21.5 and 22.3 μm, respectively, and they were separated by a 104.1-μm-wide impenetrable gap. For reasons of limitations of measurement time at the ILL high-flux reactor, the wavelength bandwidth had to be 2.8 Å which is significantly larger than that used in the earlier experiments. Figure 9 shows again the experimental results together with the first-principles theoretical calculation. The asymmetry of the diffraction pattern is fully explained by the difference of the slit widths. Here, again, we may give some simple discussion of the expected geometrical shape of the diffraction pattern. First, the envelope should correspond to the width of the single-slit diffraction pattern of Fig. 7 because the individual slits were of approximately the same width as there. Second, we may give a simple estimate of the expected separation between the double-slit interference fringes. Within the Fraunhofer approximation the angular separation

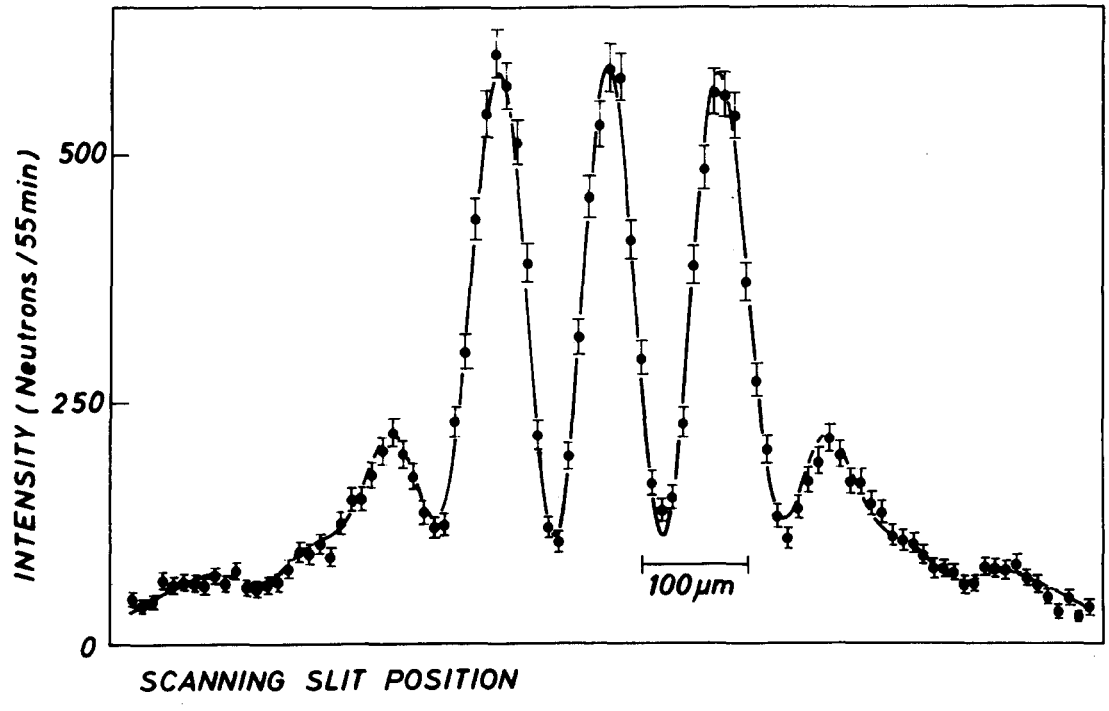

Fig. 8. Measured neutron distribution after diffraction at a double slit where a nearly transparent gold wire did serve to define the two slits.

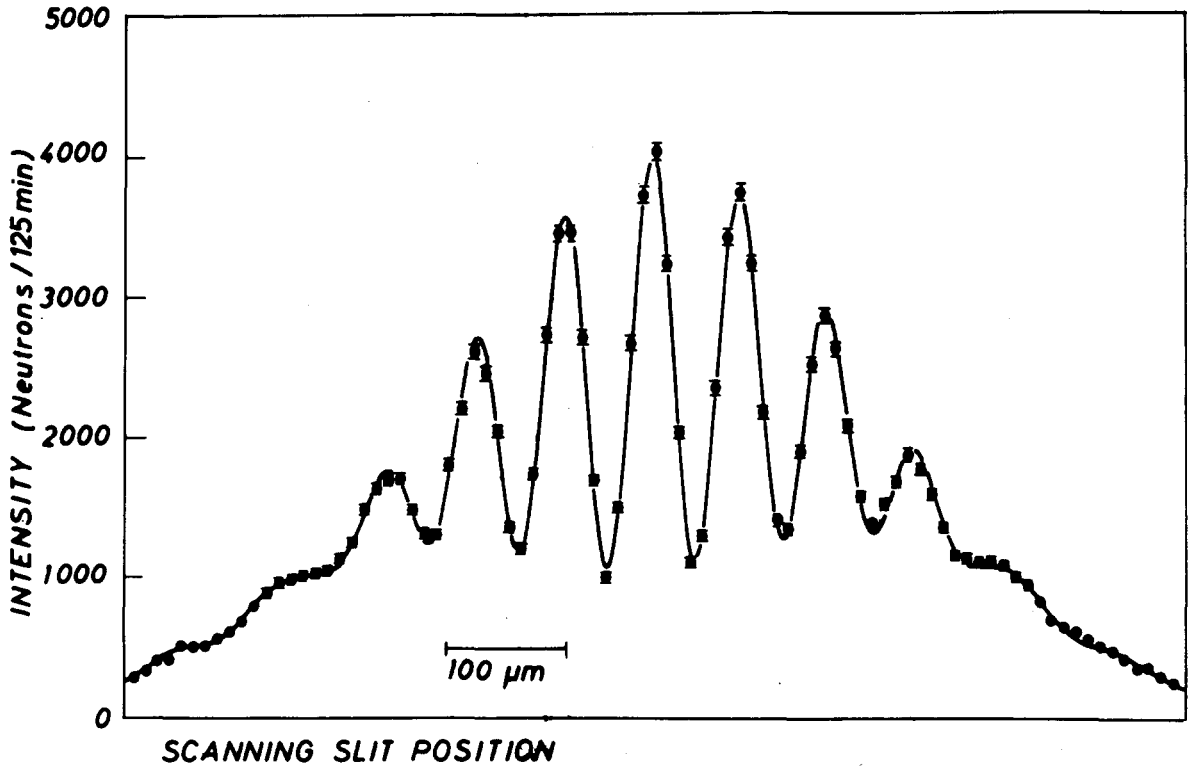

Fig. 9. Measured neutron distribution after diffraction at a double slit where a boron wire was used to define the two individual slits. The boron wire was opaque for the neutrons used in the experiment. Here, still, the solid line represents the first-principles theoretical calculation.

between two adjacent maxima is

$$\Delta\vartheta \approx \frac{\lambda}{d} = \frac{(1.85\times10^{-9}\,\mathrm{m})}{(1.26\times10^{-4}\,\mathrm{m})} = 1.5\times10^{-5}\,\mathrm{rad}$$

for small diffraction angles. Here, d is the center-to-center distance between the two diffracting slits. After a flight path of 5-m length, this translates now into a positional separation of 75 μm between the maxima. Inspection of Fig. 9 again demonstrates that both these estimates agree with experiment.

Furthermore, the fact that the diffraction pattern in Fig. 9 is not 100% modulated deserves comment. On the one hand, this observation can be explained through the broad wavelength band used. Using the numbers given above, the coherence length $L_c = \lambda^2/\Delta\lambda$ of our neutron beam was 12 nm. This implies that in the interference pattern about $n = L_c/\lambda = \lambda/\Delta\lambda \approx 7$ interference maxima should be visible until the interferences die out.[19] Again, this agrees nicely with experiment. On the other hand, even with an infinitely thin wavelength band the modulation of the double-slit pattern would not be 100% because the individual single-slit patterns do not coincide on the observation screen with slits of equal width. Therefore, 100% modulation would only be achievable in the Fraunhofer limit and with pure monochromatic radiation.[20]

VI. CONCLUDING COMMENTS

Despite the severe intensity limitations that are due to the low luminosity even of high-flux neutron sources, all the basic textbook experiments known from the optics of light have by now also been done with neutrons. One might remark that, though wave properties have already been confirmed for atoms in the 30s, neutrons to date are the heaviest particles for which precision comparison between experiment and theory of their de Broglie wave properties has been performed.

As mentioned briefly above, the low intensity implies also some interesting aspects. Inspection, for example, of Fig. 9 reveals that the highest measured intensity was about 1 neutron every 2 s. We might compare this with the time the neutrons need to traverse the distance between the nuclear reactor and the neutron detector which is of the order of 0.1 s. Taking into account that the diffusion times of the neutrons inside the nuclear reactor are even smaller, we might very well say, colloquially speaking, that, usually, while one neutron is being registered, the next neutron to be counted is still confined to its uranium nucleus.

Experiments of the kind reviewed here also provide detailed confirmations of quantum mechanics in experimental situations that are simple enough to permit a very straightforward analysis without the need of any additional assumptions which are so often necessary, even if not admitted, in experimental physics. The experiments therefore also provide evidence against possible hypothetical variants of quantum mechanics. Such variants are desired by an increasingly larger number of our theoretical colleagues working in the field of the foundations of quantum mechanics. Generally, the desire there is to resolve the famous measurement problem of quantum mechanics which, as is articulated by the Schrödinger cat paradox, may be formulated as the question why no quantum superpositions between different states of macroscopic objects are observed in nature. For the experimentalist, this can be translated into a challenging research program to exhibit quantum interference effects for increasingly larger objects and with high precision. We hope not to be too immodest by regarding our experiments as a further step along that road.

ACKNOWLEDGMENTS

The experiments reported here would have been impossible without the availability of the cold neutron sources at the Institute Laue–Langevin in Grenoble. We would like to thank the directors and staff of the ILL for continuing support. We would also like to acknowledge the collaboration with our colleagues A. G. Klein in Melbourne, W. Mampe at the ILL, C. G. Shull at MIT, and W. Treimer in Berlin. Financial support was received from the Austrian Fonds zur Förderung der wissenschaftlichen Forschung under projects No. P6635T and S42-01, from the Bundesministerium für Forschung und Technologie (Bonn), and from the US National Science Foundation (grant Nos. DMR87-13559 and INT 87-13341).

[1] C. J. Davisson and L. H. Germer, "Diffraction of electrons by a crystal of nickel," Phys. Rev. **30**, 705–740 (1927).

[2] Richard K. Gehrenbeck, "Electron diffraction: Fifty years ago," Phys. Today **31**(1), 34–41 (1978).

[3] R. Gähler, A. G. Klein, and A. Zeilinger, "Neutron optical tests of nonlinear wave mechanics," Phys. Rev. A **23**, 1611–1617 (1981); Anton Zeilinger, Roland Gähler, C. G. Shull, Wolfgang Treimer, and Walter Mampe, "Single- and double-slit diffraction of neutrons," Rev. Mod. Phys. **60**, 1067–1073 (1988).

[4] G. Möllenstedt and H. Lichte, "Electron interferometry," in *Neutron Interferometry*, edited by U. Bonse and H. Rauch (Clarendon, Oxford, 1979), pp. 363–388.

[5] G. Möllenstedt and C. Jönsson, "Elektronen-Mehrfachinterferenzen an regelmässig hergestellten Feinspalten," Z. Phys. **155**, 472–474 (1959); Claus Jönsson, "Elektroneninterferenzen an mehreren künstlich hergestellten Feinspalten," Z. Phys. **161**, 454–474 (1961); Claus Jönsson, "Electron diffraction at multiple slits," Am. J. Phys. **42**, 4–11 (1974); Gottfried Möllenstedt, "Some remarks on the quantum mechanics of the electron," Physica B **151**, 201–205 (1988).

[6] Greyson Gilson, "Demonstrations of two-slit electron interference," Am. J. Phys. **57**, 680 (1989).

[7] O. Donati, G. F. Missiroli, and G. Pozzi,"An experiment on electron interference," Am. J. Phys. **41**, 639–644 (1973); P. G. Merli, G. F. Missiroli, and G. Pozzi, "On statistical aspects of electron interference phenomena," Am. J. Phys. **44**, 306–307 (1976); G. Matteucci and G. Pozzi, "Two further experiments on electron interference," Am. J. Phys. **46**, 619–623 (1978); G. Matteucci, G. F. Missiroli, and G. Pozzi, "Electron interferometry and holography of electrostatic fields: Fundamental and applicative aspects," Physica B **151**, 223–229 (1988); Akira Tonomura, "Applications of electron holography," Rev. Mod. Phys. **59**, 639–669 (1987); A. Tonomura, J. Endo, T. Matsuda, and T. Kawasaki, "Demonstration of single-electron buildup of an interference pattern," Am J. Phys. **57**, 117–120 (1989).

[8] H. Rauch, W. Treimer, and U. Bonse, "Test of a single-crystal neutron interferometer," Phys. Lett. A **47**, 369–371 (1974); *Neutron Interferometry*, edited by U. Bonse and H. Rauch (Clarendon, Oxford, 1979).

[9] Daniel M. Greenberger, "The neutron interferometer as a device for illustrating the strange behavior of quantum systems," Rev. Mod. Phys. **55**, 875–905 (1983); G. Badurek, H. Rauch, and A. Zeilinger, "Matter wave interferometry," Proceedings of an International Workshop, Vienna 1987, Physica B **151**, 1–400 (1988).

[10] Philip M. Rinard, "Large-scale diffraction patterns from circular objects," Am. J. Phys. **44**, 70–76 (1974).

[11] G. L. Squires, *Introduction to the Theory of Thermal Neutron Scattering* (Cambridge U.P., New York, 1981).

[12] M. Born and E. Wolf, *Principles of Optics* (Pergamon, Oxford, 1980), 6th ed., p. 433.

[13] M. Born and E. Wolf, *Principles of Optics* (Pergamon, Oxford, 1980), 6th ed., p. 375.

[14] V. Drahoš and J. Komrska, "Out of focus images of spherical particles," Fourth Czechoslovak Conference on Electronics and Vacuum Physics, edited by L. Pátý (NČSAV, Prague, 1968), pp. 544–548; Jiří Komrska, "Scalar diffraction theory in electron optics," in *Advances in Electronics and Electron Physics* (Academic, New York, 1971), pp. 139–234; G. Matteucci, "Electron wavelike behavior: A historical and experimental introduction," Am. J. Phys. **58**, 1143–1147 (1990).

[15] We would like to remark that, though the geometry of our experiment was such that within our experimental resolution the Fraunhofer approximation did not quite apply, it is certainly a good enough approximation to give quantitative estimates.

[16] In our original paper, we noted some discrepancy for the slit-width values necessary to obtain an optimum fit. Specifically, the neutron slit width differed significantly from the one determined by other methods. A recent experiment (M. Tschernitz, diploma thesis, Technical University Munich, 1990, unpublished) indicates a resolution of that discrepancy. This will be published elsewhere.

[17] H. Rauch, "Scope of neutron interferometry," in *Neutron Interferometry*, edited by U. Bonse and H. Rauch (Oxford U.P., London, 1979), pp. 161–194.

[18] L. Köster and H. Rauch, "Summary of neutron scattering lengths," At. Data Nucl. Data Tables (in print).

[19] We would like to stress here that the coherence length should not be confused with the length of the neutron wave packet. The coherence length is strictly defined operationally via the optical path difference until interference fringes disappear or, in more practical terms, until the interference fringe contrast reduces to a certain fraction, say $1/2$ or $1/e$, of its maximum value. The coherence length therefore is just a function of the wavelength distribution in the beam and it does not change upon propagation through free space. In contrast, the length of the wave packet also depends on the relative phases between different wavelength components and, therefore, it is not a constant as evidenced by the famous spreading of wave packets. It is easy to estimate that in our experiment a wave packet starting with minimal size, i.e., the coherence length, at the entrance to the apparatus would spread to a length of the order of 1 m at its end. We are not aware of any experiment that would have directly measured the length of a wave packet and not just the coherence length of a beam. For discussions of these questions, see: H. Kaiser, S. A. Werner, and E. A George, "Direct measurement of the longitudinal coherence length of a thermal neutron beam," Phys. Rev. Lett. **50**, 560–563 (1983); A. G. Klein, G. I. Opat, and W. A. Hamilton, "Longitudinal coherence in neutron interferometry," Phys. Rev. Lett. **50**, 563–565 (1983); G. Comsa, "Comment on: Direct measurement of the longitudinal coherence length of a thermal neutron beam," Phys. Rev. Lett. **51**, 1105 (1983); H. Kaiser, S. A. Werner, and E. A. George, "Reply to Comsa's comment," Phys. Rev. Lett. **51**, 1106 (1983); H. J. Bernstein and F. E. Low, "Measurement of longitudinal coherence lengths in particle beams," Phys. Rev. Lett. **59**, 951–953 (1987).

[20] In our experiment the rotation of the Earth did lead to a deflection of the interference patterns observed through the action of the Coriolis force or, quantum mechanically, the Sagnac effect. Since this deflection is a function of neutron wavelength, it also leads to a reduction of the interference contrast if nonmonochromatic radiation is used. For our case the mean deflection was of the order of 13 μm and its consequence on the interference contrast just too small for observation.